

One Channel to Rule Them All: Rethinking Input Representation for Visual Place Recognition

Timur Ismagilov^{1*}, Shakaiba Majeed², Michael Milford³, Tan Viet Tuyen Nguyen¹
Sarvapali D. Ramchurn¹, Shoaib Ehsan^{1,4}

Abstract—Visual Place Recognition (VPR) is fundamental to long-term robot localization and SLAM, yet current systems overwhelmingly rely on RGB input, implicitly assuming color is necessary for global place recognition. We challenge this assumption, investigating the role of chromatic information across training regimes, model architectures and standard benchmarks under real-world appearance variation. We find that grayscale matches RGB performance generally and outperforms it under severe appearance shifts where color invariance is insufficiently learned, while color provides meaningful gains only where persistent and discriminative chromatic cues are present. Across selected benchmarks, a fully gray-trained MixVPR model achieves an average 82.4% Recall@1 compared to 81.2% for its RGB counterpart. In some cases, lightweight grayscale variants with 60% fewer parameters can outperform heavier RGB models. Grayscale further offers practical advantages in storage, bandwidth and alignment with resource-constrained systems. We conclude that for global VPR where scenes vary across illumination, weather, season and setting, color contributes minimally, and grayscale alone is sufficient for reliable place recognition.

I. INTRODUCTION

VISUAL Place Recognition (VPR) is a core component of mobile robotics, enabling navigation and loop-closure detection for Simultaneous Localization And Mapping (SLAM). Unlike object-centric tasks that focus on local discriminative cues for detection or recognition, VPR operates on global scene representations, encoding broad spatial context into compact descriptors. State-of-the-Art (SotA) VPR methods predominantly rely on color imagery, inheriting the conventions of foundational models like ResNet and DINOv2 which provide robust low-level features transferred from large-scale training on ImageNet and LVD-142M datasets. The assumption that color input is required for VPR has become ubiquitous despite limited evaluation of its contribution to performance or its practical implications within VPR systems.

Recognizing the same place under severe perceptual aliasing is a fundamental challenge in VPR. Appearance changes,

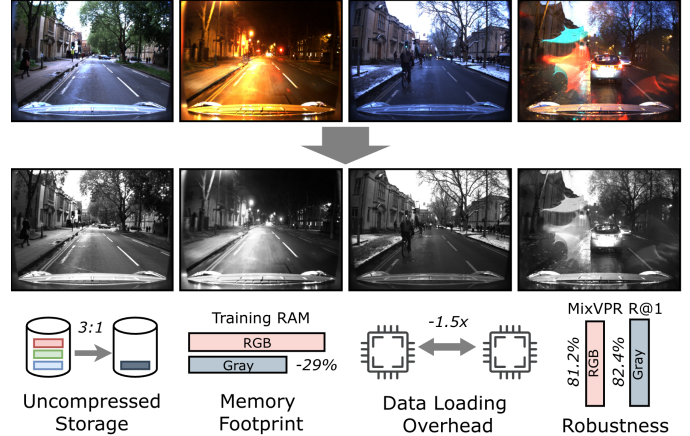


Fig. 1. We investigate the role of color in VPR, examining its impact on retrieval performance across appearance conditions and the practical considerations of grayscale input for training and deployment.

including seasonal shifts, weather, illumination, camera viewpoint, dynamic objects and long-term structural changes, require robust models capable of broad generalization. Among these, color variation introduces a degree of freedom that, without sufficient representation during training, can degrade model performance. In contrast, grayscale imagery is centered on luminance-based structure, which may offer more robust place representations under such conditions, while also reducing the input dimensionality, storage requirements for data, and memory utilization across training and inference pipelines. Despite this, the reliance on RGB input in modern VPR architectures remains largely unexamined. Current VPR approaches operate on RGB input driven by the design of their pretrained backbones [1]–[6], yet this raises the question of whether color is fundamentally necessary for localization, and whether such models remain susceptible to color-shift induced degradation. Additionally, VPR datasets are almost exclusively stored, trained and evaluated in RGB format [7]–[9], leaving potential gains in data efficiency, memory footprint and edge deployability largely unexplored.

The role of color in both nature and computer vision is widely investigated. Evidence from both suggests its utility is task and data-dependent. In object-centric studies, color imagery has been shown to benefit the classification of faces, edges and object categories such as food [10]–[14]. Other works report more nuanced findings, such as indifference in deep face recognition [15], over-sensitivity to hue shifts [11], grayscale superiority on texture-dominant data [16] and broader effects on human perception such as memory retrieval and decision-making under degraded conditions [17]–[20].

*Corresponding author.

¹Timur Ismagilov, Tan Viet Tuyen Nguyen, Sarvapali D. Ramchurn and Shoaib Ehsan are with the School of Electronics and Computer Science, University of Southampton, SO17 1BJ Southampton, U.K. tile24@soton.ac.uk, tuyen.nguyen@soton.ac.uk, sdr1@soton.ac.uk, s.ehsan@soton.ac.uk

²Shakaiba Majeed is with the Department of Computer Science and Engineering, Hanyang University, Seoul, South Korea. shakaiba33@hanyang.ac.kr

³Michael Milford is with the QUT Centre for Robotics, School of Electrical Engineering and Robotics, Brisbane, QLD 4000, Australia. michael.milford@qut.edu.au

⁴Shoaib Ehsan is also with the School of Computer Science and Electronic Engineering, University of Essex, Colchester, CO4 3SQ, U.K. sehsan@essex.ac.uk

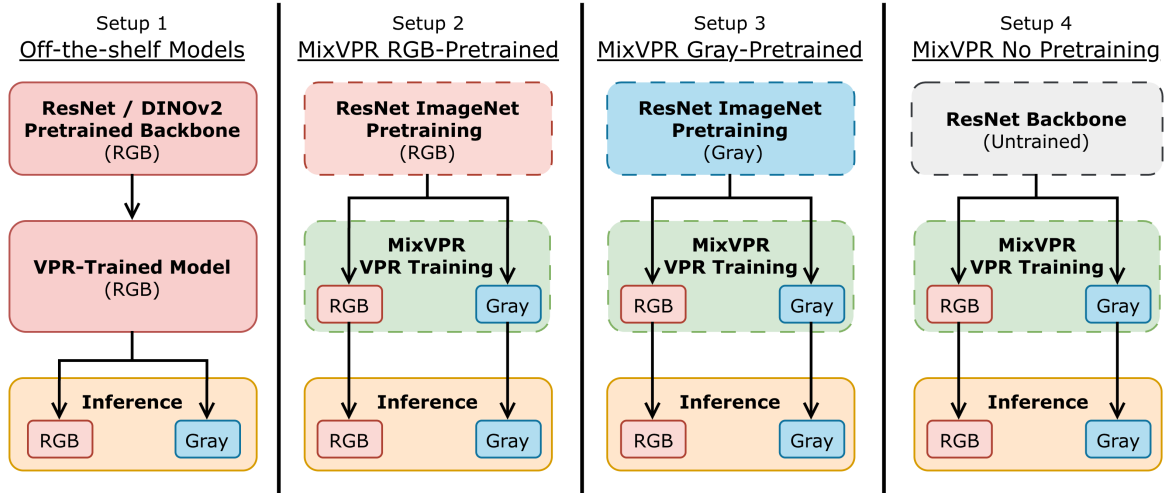


Fig. 2. Overview of experimental setups. Setup 1 evaluates off-the-shelf RGB-trained models directly. Setups 2 & 3 fine-tune MixVPR on GSV-Cities using RGB and grayscale-pretrained ResNet backbones respectively, across both modalities. Setup 4 trains MixVPR from scratch without ImageNet pretraining, also across both modalities. All MixVPR training uses identical hardware, hyperparameters and data splits.

TABLE I
OFF-THE-SHELF VPR MODELS EVALUATED IN THIS WORK.

Model	Backbone	Pretrain	VPR Train	Params	Dim
EigenPlaces [1]	ResNet-50	ImageNet	SF-XL	27.7M	2048
MixVPR [4]	ResNet-50	ImageNet	GSV-Cities	10.9M	4096
CricaVPR [5]	ViT-B/14	LVD-142M	GSV-Cities	106.8M	10752
SALAD [21]	ViT-B/14	LVD-142M	GSV-Cities	88.0M	8448
BoQ [22]	ViT-B/14	LVD-142M	GSV-Cities	95.2M	12288

Within robotic vision, the role of color in VPR has received comparatively little attention. Given the appearance variability inherent to real-world deployment, where color can be a distractor rather than a discriminative signal, we question whether three-channel color input is strictly necessary for VPR with existing models. We make the following contributions:

- An evaluation of RGB and grayscale imagery across SotA models. We find that recent off-the-shelf RGB-trained models show only marginal benefit from color, suggesting that the VPR objective is largely structure and luminance-driven, with color providing marginal support only where consistent chromatic cues are present.
- An empirical investigation of the role of color in VPR under different training regimes using MixVPR. When controlling for training, grayscale achieves competitive performance generally and outperforms RGB under challenging appearance shifts, exposing insufficient color invariance in current training conventions.
- A discussion of practical advantages with grayscale input, including reduced storage, data-loading overhead and memory footprint, alongside its suitability for resource-constrained deployment and embedded sensor modalities.

The rest of the paper is organized as follows: Section II provides an overview of VPR literature and color in recognition tasks. Section III outlines our experimental setup. Results are presented and discussed in Section IV and Section V. Finally, we conclude and discuss future work in Section VI.

II. RELATED WORK

Visual Place Recognition. Retrieval-based VPR represents places as compact feature descriptors, using nearest-neighbor retrieval for localization. Early approaches extracted hand-crafted local features from grayscale imagery (SIFT [23], ORB [24]), aggregated into global representations via VLAD [25], BoW [26] or GeM [27]. Deep learning methods have largely superseded these. MixVPR [4] uses ResNet50 with channel feature mixing. CosPlace [2] and EigenPlaces [1] both use ResNet50 with GeM pooling, differing in their scene partitioning strategy. More recent ViT-based models show stronger retrieval performance: CricaVPR [5] applies a DINOv2 backbone with cross-image correlation. SALAD [21] reformulates NetVLAD’s [3] soft-assignment as optimal transport on DINOv2 features. BoQ [22] uses learnable global queries with cross-attention, and MegaLoc [6] combines diverse training strategies on a SALAD architecture. Training efficiency is addressed via hard data sampling strategies: CliqueMining [28] constructs a geographic-descriptor graph to sample hard image pairs, and Global Proxy Mining (GPM) [29] uses training proxy descriptors for hard batch construction.

Despite increasing performance over time, the role of color in VPR has received little attention. RGB has been adopted by default with pretrained backbones, yet neither ResNet’s object-centric ImageNet supervision nor DINOv2’s self-supervised pretraining is guaranteed to capture chromatic variability at VPR inference. Practically, grayscale reduces uncompressed storage by two-thirds relative to RGB, which is significant for terabyte-scale datasets, and proportionally reduces host-to-device transfer, improving training efficiency [15]. Edge deployment and TinyML platforms [30] operate under tight memory budgets, and even lightweight vSLAM and VPR pipelines have required offline preprocessing to meet real-time constraints on resource-constrained platforms [31], [32].

Impact of Color in Vision Tasks. Color utility is largely task and data-dependent in both human and machine vision. In human vision, color supports object recognition [12], face recognition [13], [19], and edge classification [14], yet scene

TABLE II
RECALL@1 ACROSS NORDLAND SEASON PAIRS, EVALUATED ON RGB AND GRAY USING OFF-THE-SHELF MODELS.

Reference ↓	Model →	EigenPlaces				MixVPR				SALAD				CricaVPR				BoQ			
	Query → Eval. Mode ↓	Fall	Spring	Summer	Winter	Fall	Spring	Summer	Winter	Fall	Spring	Summer	Winter	Fall	Spring	Summer	Winter	Fall	Spring	Summer	Winter
Fall	RGB	—	89.0	93.5	63.1	—	95.4	95.9	81.7	—	97.4	97.3	88.9	—	98.6	98.4	96.1	—	97.9	97.2	93.0
	Gray	—	81.1	90.3	53.4	—	93.3	94.2	80.3	—	96.7	96.4	87.7	—	98.2	97.8	94.1	—	97.4	97.0	91.4
Spring	RGB	80.5	—	73.1	68.5	88.1	—	83.2	89.4	95.0	—	93.0	92.2	98.0	—	95.8	98.3	96.2	—	94.7	95.6
	Gray	70.0	—	64.2	59.6	84.7	—	80.8	89.8	94.5	—	91.4	93.4	97.6	—	93.7	97.5	96.4	—	93.4	96.2
Summer	RGB	94.4	82.7	—	60.1	95.8	91.6	—	78.3	97.6	94.9	—	86.8	98.1	96.9	—	94.5	97.4	95.7	—	89.9
	Gray	91.3	76.8	—	51.1	94.0	89.1	—	76.4	97.3	93.5	—	85.6	97.9	96.0	—	92.8	97.2	95.2	—	89.4
Winter	RGB	52.0	71.1	47.3	—	70.5	86.9	65.6	—	86.9	93.9	84.5	—	93.6	97.4	92.4	—	89.6	96.7	88.6	—
	Gray	43.6	62.9	39.8	—	67.5	84.1	64.3	—	86.6	93.7	83.9	—	92.3	97.4	90.5	—	90.4	96.7	88.7	—
Avg. ΔR@1 (RGB–Gray)		7.6				2.0				0.6				1.0				0.3			

TABLE III
RECALL@1 ACROSS OXFORD ROBOTCAR WEATHER PAIRS, EVALUATED ON RGB AND GRAY USING OFF-THE-SHELF MODELS.

Reference ↓	Model →	EigenPlaces						MixVPR						SALAD						CricaVPR						BoQ					
	Query → Eval. Mode ↓	Sun	Dusk	Overcast	Rain	Night	Snow	Sun	Dusk	Overcast	Rain	Night	Snow	Sun	Dusk	Overcast	Rain	Night	Snow	Sun	Dusk	Overcast	Rain	Night	Snow	Sun	Dusk	Overcast	Rain	Night	Snow
Sun	RGB	—	59.3	96.7	94.8	44.8	87.4	—	64.3	97.4	96.9	66.3	90.4	—	71.4	96.6	95.8	83.5	89.4	—	72.0	97.1	96.6	81.5	89.3	—	77.5	98.0	97.4	89.8	90.9
	Gray	—	51.4	96.2	93.4	42.5	86.6	—	57.9	95.4	94.7	68.3	85.1	—	67.9	96.1	95.1	82.6	86.7	—	68.6	97.1	96.6	80.5	87.9	—	75.4	97.8	97.1	89.4	89.0
Dusk	RGB	54.4	—	55.5	50.4	37.1	58.0	58.2	—	57.7	52.6	51.9	59.6	66.7	—	66.5	62.3	71.1	67.1	66.3	—	67.4	62.7	69.2	67.7	75.0	—	75.9	68.3	75.8	72.6
	Gray	47.3	—	49.0	43.5	30.3	49.3	53.3	—	53.7	49.0	48.1	56.4	64.4	—	64.3	58.3	65.8	63.4	62.7	—	65.6	60.6	65.2	65.5	73.7	—	73.5	65.0	71.7	70.3
Overcast	RGB	96.5	60.0	—	94.2	50.5	89.7	96.7	67.0	—	95.8	72.5	91.3	96.2	72.4	—	94.8	84.7	90.3	96.7	72.9	—	95.9	83.0	91.0	97.4	80.2	—	96.5	91.6	92.8
	Gray	96.6	53.2	—	93.7	47.7	89.2	96.0	60.1	—	95.1	73.7	87.4	96.4	69.0	—	95.1	85.5	89.4	96.7	71.7	—	95.7	81.5	90.7	97.2	78.5	—	96.4	90.8	91.5
Rain	RGB	95.5	55.1	95.0	—	46.8	85.8	95.8	57.6	95.2	—	65.7	85.8	94.7	64.0	95.5	—	83.1	87.2	96.2	67.7	95.0	—	81.5	86.4	96.8	71.2	96.9	—	88.8	89.3
	Gray	94.0	47.0	93.7	—	40.4	84.4	94.8	52.1	94.4	—	64.9	82.9	95.7	61.4	95.3	—	82.1	85.7	96.7	65.0	96.0	—	80.4	86.3	96.9	67.7	97.3	—	87.0	88.2
Night	RGB	64.8	47.8	70.2	61.7	—	61.2	71.1	60.2	74.4	70.3	—	70.5	80.8	71.8	80.2	80.0	—	78.6	81.8	70.6	82.9	80.8	—	77.5	88.9	77.2	89.6	87.1	—	84.0
	Gray	61.2	42.6	64.8	55.7	—	56.8	71.1	53.2	74.4	70.6	—	65.4	83.8	68.4	84.2	81.1	—	79.3	81.3	69.0	84.7	81.4	—	78.7	88.0	76.2	88.8	86.8	—	85.2
Snow	RGB	89.9	66.7	93.0	88.4	52.3	—	92.5	71.5	94.4	90.4	71.0	—	92.0	72.7	93.4	89.9	83.7	—	92.9	77.5	94.4	90.8	83.8	—	93.7	79.5	95.5	92.0	88.8	—
	Gray	89.2	57.4	92.3	87.2	50.6	—	88.8	65.7	92.0	86.9	65.2	—	90.2	71.4	93.6	89.5	83.8	—	91.6	73.8	94.3	90.5	82.2	—	93.2	78.1	95.1	91.5	89.3	—
Avg. ΔR@1 (RGB–Gray)		3.9						2.9						1.0						1.0						1.1					

TABLE IV
RECALL@1 ACROSS DATASETS, EVALUATED ON RGB AND GRAY USING OFF-THE-SHELF MODELS.

Model	Eval. Mode	Pitts250k (Test)	SPED	GLDv2	Tokyo247	Avg.ΔR@1 (RGB-Gray)
EigenPlaces	RGB	95.1	78.2	53.6	80.6	3.4
	Gray	94.4	75.4	51.0	73.0	
MixVPR	RGB	96.0	84.7	59.5	86.4	5.0
	Gray	93.8	86.5	53.8	72.4	
SALAD	RGB	97.4	92.1	71.7	94.6	2.1
	Gray	96.7	90.9	67.7	92.1	
CricaVPR	RGB	96.2	92.9	70.2	93.0	1.3
	Gray	95.6	92.9	67.7	90.8	
BoQ	RGB	97.6	92.6	74.2	96.5	1.2
	Gray	97.6	91.4	71.0	96.2	

recognition studies show it does not consistently improve accuracy, instead contributing to memory retrieval and decision latency [17], [33]. Spatial structure primarily drives real-world visual search [20], and early scene categorization is largely unaffected by color absence [18]. Late-sighted individuals exhibit over-reliance on color [11], implicating luminance-based structure as the foundation for robust learning. In computer vision, color aids object-centric recognition [10], [11] but has little effect on face recognition under grayscale [15]. Luminance-based structure is more robust to color space changes and advantageous in texture-dominant settings [16]. At the representation level, color sensitivity was found to concentrate in early layers of CNNs and diminishing as features become class-specific [34]. Surrounding object-centric data, ColorSense [35] finds that performance gaps between color-contrast difficulty groups persist regardless of architecture or

augmentation, with grayscale only partially reducing bias, and [36] highlight that RGB-trained models degrade significantly under chromatic shifts, yet color’s role in VPR for robotics and mobile deployment remains underexplored. Unlike such tasks, VPR requires globally consistent representations across severe appearance and structural change. Existing evaluations address appearance variation, viewpoint change and degradation from architectural and loss perspectives [37]–[40], with limited analysis of color-induced variation. Under illumination, weather and seasonal shifts, color is unstable and can harm retrieval if models lack invariance. This raises the question of whether structural and texture cues alone suffice, and whether grayscale representations offer lower-variance, robust alternatives with reduced overhead.

III. EXPERIMENTAL METHODOLOGY

We evaluate the impact of color on VPR across architectures and training regimes, structured into setups shown in Fig. 2.

Setup 1: Off-the-shelf. Existing VPR models (Table I) are evaluated without modification, covering ResNet-based (EigenPlaces, MixVPR) and DINOv2-based methods (SALAD, CricaVPR, BoQ), all RGB pretrained and VPR-trained. Each is evaluated on both RGB and grayscale benchmarks. For grayscale, the single image channel is replicated across three to match the model input format.

Setups 2 & 3: Controlled Training. We isolate MixVPR for its simplicity and lightweight design. DINOv2-based models are excluded as LVD-142M is unavailable for replication.

TABLE V
RECALL@1 ACROSS NORDLAND SEASON PAIRS WITH MIXVPR TRAINED & EVALUATED PER MODALITY, RGB IMAGENET PRETRAINED.

Reference ↓	Model →	MixVPR – ResNet18				MixVPR – ResNet34				MixVPR – ResNet50			
	Query →	Fall	Spring	Summer	Winter	Fall	Spring	Summer	Winter	Fall	Spring	Summer	Winter
	Mode ↓												
Fall	RGB	—	94.3	94.7	75.3	—	91.8	94.5	71.5	—	95.6	95.5	82.7
	Gray	—	92.7	94.3	74.9	—	91.6	93.6	74.1	—	94.9	95.0	83.5
Spring	RGB	87.9	—	80.6	84.0	83.7	—	77.6	82.0	89.9	—	84.4	89.7
	Gray	85.5	—	78.6	86.7	83.5	—	78.5	86.2	89.2	—	84.0	92.9
Summer	RGB	94.8	88.8	—	73.0	95.0	88.8	—	70.5	96.1	91.3	—	80.4
	Gray	94.1	86.9	—	72.9	93.7	87.6	—	70.6	95.2	91.1	—	80.8
Winter	RGB	64.7	82.9	60.9	—	59.0	78.6	56.7	—	74.9	88.5	70.3	—
	Gray	66.8	83.8	63.6	—	63.3	82.1	61.8	—	76.2	89.8	73.0	—
Avg. $\Delta R@1$ (RGB–Gray)		0.1				-1.4				-0.5			

TABLE VI
RECALL@1 ACROSS OXFORD ROBOTCAR WEATHER PAIRS WITH MIXVPR TRAINED & EVALUATED PER MODALITY, RGB IMAGENET PRETRAINED.

Reference ↓	Model →	MixVPR – ResNet18						MixVPR – ResNet34						MixVPR – ResNet50					
	Query →	Sun	Dusk	Overcast	Rain	Night	Snow	Sun	Dusk	Overcast	Rain	Night	Snow	Sun	Dusk	Overcast	Rain	Night	Snow
	Mode ↓																		
Sun	RGB	—	57.9	96.5	95.3	50.0	87.3	—	59.2	96.8	95.0	58.4	87.9	—	65.8	97.5	96.5	67.5	90.4
	Gray	—	60.3	97.0	95.2	65.4	88.5	—	63.4	97.0	96.2	71.3	89.0	—	69.0	97.4	96.7	78.9	90.6
Dusk	RGB	54.1	—	53.7	51.1	38.4	58.0	55.7	—	56.1	52.6	47.6	57.9	55.7	—	56.5	53.1	53.1	59.8
	Gray	54.1	—	55.6	51.2	52.6	58.9	57.0	—	58.0	52.0	54.9	58.6	60.7	—	61.0	54.8	61.2	62.7
Overcast	RGB	96.4	59.4	—	94.6	52.9	89.4	96.2	60.5	—	94.2	61.9	89.7	96.9	65.6	—	96.0	69.2	91.7
	Gray	96.6	61.4	—	94.9	69.1	90.9	95.9	63.6	—	95.1	74.3	91.9	97.3	71.0	—	96.4	83.2	93.0
Rain	RGB	93.4	53.7	93.0	—	46.9	82.4	94.1	54.2	93.6	—	53.9	82.8	95.4	56.1	94.8	—	62.0	85.8
	Gray	96.0	53.2	94.7	—	61.5	84.6	95.6	56.6	95.4	—	68.2	85.9	96.9	60.9	96.6	—	74.2	87.2
Night	RGB	55.0	49.6	57.7	53.9	—	54.1	61.1	53.2	65.9	58.2	—	60.8	68.0	57.7	71.4	66.3	—	66.7
	Gray	70.0	56.1	73.2	67.3	—	67.2	75.0	60.2	77.8	72.0	—	72.5	78.7	66.6	82.7	77.8	—	78.3
Snow	RGB	89.2	67.3	92.6	87.4	53.1	—	90.7	67.5	92.8	86.8	60.8	—	92.8	71.8	94.8	90.8	69.7	—
	Gray	91.2	68.9	93.2	88.2	67.2	—	91.4	69.3	94.0	88.7	72.8	—	92.3	75.7	95.1	91.3	81.3	—
Avg. $\Delta R@1$ (RGB–Gray)		-5.3						-4.9						-5.0					

TABLE VII
RECALL@1 ACROSS DATASETS WITH MIXVPR TRAINED & EVALUATED PER MODALITY, RGB IMAGENET PRETRAINED.

Model	Mode	Pitts250k (Test)	SPED	GLDv2	Tokyo247	Avg. $\Delta R@1$ (RGB-Gray)
MixVPR (ResNet18)	RGB	94.0	82.2	51.1	74.0	0.2
	Gray	93.6	84.2	49.4	73.3	
MixVPR (ResNet34)	RGB	94.8	82.5	53.3	79.4	1.7
	Gray	94.9	84.7	49.7	74.0	
MixVPR (ResNet50)	RGB	96.4	83.7	58.9	86.4	0.1
	Gray	96.0	85.3	57.1	86.4	

ResNet backbones are pretrained on RGB and grayscale ImageNet from scratch, then fine-tuned and evaluated on either modality, yielding four variants across ResNet18, 34 and 50. All experiments share the same seed, hardware and hyperparameters. The full model is kept unfrozen during VPR fine-tuning. RGB input weights are averaged to one channel for grayscale fine-tuning, and grayscale input weights are replicated across three for RGB.

Setup 4: VPR Training from Scratch. MixVPR is trained directly on VPR data without ImageNet pretraining across both modalities and all three backbone sizes, isolating color’s role in the VPR objective and examining whether GSV-Cities provides sufficient color invariance for generalization.

Datasets. Models are evaluated on six benchmarks covering seasonal, weather, illumination and viewpoint change.

1) **Nordland:** A 729km railway traverse in Norway

recorded across spring, summer, fall and winter, evaluating performance under seasonal change. We regularly sample each season traverse to 3,975 frames and remove stationary and tunnel segments.

- 2) **Oxford RobotCar:** Car traverses under six chosen conditions (sun, dusk, rain, overcast, night, snow). We establish 4,054 frame-to-frame correspondences per set at approximately 1m spatial sub-sampling.
- 3) **Pitts250k-Test:** 3,498 urban city locations, each with 12 images at 30° intervals. 1000 random queries are sampled, assessing viewpoint and illumination robustness.
- 4) **SPED-Test:** Consists of mixed outdoor scenes captured from fixed cameras under significant illumination, weather, season and viewpoint changes. We use 608 reference-query pairs with one-to-one correspondences.
- 5) **Google Landmarks Dataset (GLDv2):** A landmark-focused benchmark with 23,294 reference and 3,103 queries exhibiting viewpoint, scale and appearance variation, reflecting uncontrolled acquisition.
- 6) **Tokyo24/7:** 6,334 reference locations in Tokyo, each with 12 images at 30° intervals, and 105 query triplets, each containing day, evening and night variants under dense structural change.

Retrieval. Performance is measured with Recall@1, defined by the proportion of queries where the top retrieved image falls

TABLE VIII
RECALL@1 ACROSS NORDLAND SEASON PAIRS WITH MIXVPR TRAINED & EVALUATED PER MODALITY, GRAY IMAGENET PRETRAINED.

Reference ↓	Model →	MixVPR – ResNet18				MixVPR – ResNet34				MixVPR – ResNet50			
	Query →	Fall	Spring	Summer	Winter	Fall	Spring	Summer	Winter	Fall	Spring	Summer	Winter
	Mode ↓												
Fall	RGB	—	94.2	94.6	75.9	—	91.8	94.4	73.2	—	95.1	95.8	82.6
	Gray	—	93.4	94.0	76.4	—	92.8	93.8	73.6	—	95.4	95.4	82.6
Spring	RGB	86.9	—	80.1	85.6	83.1	—	78.6	82.0	88.0	—	82.5	89.7
	Gray	89.9	—	83.6	88.2	85.6	—	80.4	85.8	90.5	—	85.4	91.6
Summer	RGB	95.1	89.3	—	73.0	93.9	87.9	—	70.5	96.1	91.0	—	78.3
	Gray	94.3	88.5	—	73.5	93.8	88.7	—	71.7	95.7	91.3	—	78.9
Winter	RGB	67.8	84.1	64.2	—	63.0	81.3	61.0	—	70.9	87.5	66.4	—
	Gray	69.7	84.8	66.6	—	65.0	84.3	62.3	—	75.5	89.8	71.0	—
Avg. $\Delta R@1$ (RGB–Gray)		-1.0				-1.4				-1.6			

TABLE IX
RECALL@1 ACROSS OXFORD ROBOTCAR WEATHER PAIRS WITH MIXVPR TRAINED & EVALUATED PER MODALITY, GRAY IMAGENET PRETRAINED.

Reference ↓	Model →	MixVPR – ResNet18						MixVPR – ResNet34						MixVPR – ResNet50					
	Query →	Sun	Dusk	Overcast	Rain	Night	Snow	Sun	Dusk	Overcast	Rain	Night	Snow	Sun	Dusk	Overcast	Rain	Night	Snow
	Mode ↓																		
Sun	RGB	—	58.7	96.9	95.8	49.4	87.9	—	59.3	97.1	95.0	54.9	88.8	—	64.9	97.4	96.7	68.4	89.5
	Gray	—	60.0	97.0	96.0	67.2	88.9	—	60.9	97.0	96.0	72.5	88.4	—	66.4	97.2	96.7	79.8	89.9
Dusk	RGB	53.8	—	54.5	51.8	40.7	57.2	53.8	—	52.0	50.4	45.3	59.3	56.9	—	56.4	53.5	54.0	59.6
	Gray	54.7	—	55.1	50.8	54.0	58.0	53.3	—	54.3	49.8	53.9	57.6	58.5	—	59.6	54.3	60.2	61.0
Overcast	RGB	96.4	60.2	—	95.1	53.4	90.3	96.4	61.3	—	95.7	60.4	90.5	97.3	66.5	—	96.3	74.2	92.5
	Gray	96.8	63.6	—	96.2	74.0	91.0	96.6	62.1	—	96.1	77.2	91.7	97.3	68.3	—	96.9	83.4	92.8
Rain	RGB	94.9	52.0	93.8	—	46.5	82.9	94.7	54.6	94.1	—	51.5	84.1	96.7	58.1	95.9	—	64.7	87.1
	Gray	95.5	54.8	95.2	—	63.8	85.0	95.8	54.4	95.4	—	68.9	85.5	97.0	61.2	96.5	—	75.9	87.5
Night	RGB	54.8	47.5	60.5	56.0	—	55.0	57.8	53.3	62.2	57.8	—	59.1	70.1	60.9	74.5	67.4	—	68.2
	Gray	72.2	55.9	77.1	69.1	—	69.5	72.9	58.2	77.7	70.4	—	70.8	79.2	66.7	83.7	77.1	—	77.8
Snow	RGB	90.3	67.2	93.6	86.8	55.3	—	90.3	67.7	93.0	87.7	59.7	—	92.7	72.0	95.1	90.6	71.4	—
	Gray	90.7	69.0	94.0	88.1	72.8	—	91.8	67.0	93.2	88.5	72.5	—	93.8	74.0	95.6	90.7	80.3	—
Avg. $\Delta R@1$ (RGB–Gray)		-5.9						-4.7						-3.7					

TABLE X
RECALL@1 ACROSS DATASETS WITH MIXVPR TRAINED & EVALUATED PER MODALITY, GRAY IMAGENET PRETRAINED.

Model	Mode	Pitts250k (Test)	SPED	GLDv2	Tokyo247	Avg. $\Delta R@1$ (RGB-Gray)
MixVPR (ResNet18)	RGB	94.1	82.7	50.3	74.9	-0.1
	Gray	93.5	83.7	48.8	76.2	
MixVPR (ResNet34)	RGB	94.8	84.2	51.5	76.2	-0.3
	Gray	95.0	84.0	51.5	77.5	
MixVPR (ResNet50)	RGB	95.4	85.8	57.5	86.7	-0.6
	Gray	95.5	87.6	57.9	86.7	

within the ground truth tolerance: 5m for Oxford RobotCar, 25m for Pitts250k and Tokyo24/7, one-to-one correspondence for Nordland and SPED, and provided labels for GLDv2. All training uses an Nvidia A100 GPU with fixed seeds.

IV. ANALYSIS OF RESULTS

1) Off-the-shelf Performance. Tables II to IV report the performance of off-the-shelf models on RGB and grayscale versions of each benchmark. We find that the more recent transformer-based models exhibit a significantly smaller performance gap between RGB and gray retrieval, with EigenPlaces achieving an average 7.6% Recall@1 improvement on Nordland using RGB, while BoQ, on average, only differs by 0.3%. This is interesting, given the models have been entirely trained on RGB imagery, yet the apparent utility of color to VPR itself is limited. We suspect that EigenPlaces

and MixVPR develop a greater reliance on chromatic features under ImageNet training and are unable to adapt across color space, while the DINOv2-based models are sufficiently appearance-invariant through their self-supervised pre-training that color proves to be more redundant for VPR. However, certain conditions in weather or datasets appear to consistently benefit under RGB across the models, such as GLDv2 by $\approx 3\%$, suggesting that color may indeed provide some discriminative value when stable chromatic cues are present (GLDv2 is landmark-focused under broadly consistent lighting). Nevertheless, the overall trend suggests that luminance-based structure largely dominates stable global place recognition.

2) RGB-Pretrained MixVPR. When controlling for VPR fine-tuning (see Tables V to VII), the performance gap between RGB and grayscale VPR narrows considerably and often reverses in favor of grayscale. While off-the-shelf MixVPR shows more reliance on color, this advantage largely disappears with grayscale VPR fine-tuning, with the model able to perform well under both color spaces and even outperforming RGB under more severe appearance shifts. For example, MixVPR-ResNet50 achieves 82.7% R@1 on Oxford RobotCar (night reference, overcast query) under grayscale, compared to 71.4% for the RGB equivalent, as well as outperforming the off-the-shelf model, indicating that its RGB training fails to achieve full color invariance un-

TABLE XI
RECALL@1 ACROSS NORDLAND SEASON PAIRS WITH MIXVPR TRAINED & EVALUATED ON THE SAME MODALITY, WITHOUT PRETRAINING.

Reference ↓	Model →	MixVPR - ResNet18				MixVPR - ResNet34				MixVPR - ResNet50			
	Query →	Fall	Spring	Summer	Winter	Fall	Spring	Summer	Winter	Fall	Spring	Summer	Winter
	Mode ↓												
Fall	RGB	—	88.3	92.3	62.1	—	86.1	92.5	59.7	—	83.2	90.8	52.9
	Gray	—	89.3	94.2	64.9	—	87.0	93.0	61.8	—	86.2	92.5	56.5
Spring	RGB	78.3	—	67.5	67.3	75.8	—	66.9	66.0	73.7	—	64.9	56.1
	Gray	82.2	—	75.7	78.7	79.2	—	73.1	75.8	76.7	—	68.4	70.9
Summer	RGB	93.5	81.4	—	58.9	93.1	80.5	—	57.3	92.6	79.0	—	50.9
	Gray	94.0	83.9	—	64.6	92.4	81.6	—	62.0	92.5	79.8	—	54.9
Winter	RGB	49.0	64.4	44.1	—	52.9	68.3	49.2	—	39.4	53.3	36.2	—
	Gray	60.8	75.9	58.2	—	56.2	74.7	56.5	—	47.3	68.2	45.9	—
Avg. ΔR@1 (RGB-Gray)		-6.3				-3.8				-5.6			

TABLE XII
RECALL@1 ACROSS OXFORD ROBOTCAR WEATHER PAIRS WITH MIXVPR TRAINED & EVALUATED ON THE SAME MODALITY, WITHOUT PRETRAINING.

Reference ↓	Model →	MixVPR - ResNet18						MixVPR - ResNet34						MixVPR - ResNet50					
	Query →	Sun	Dusk	Overcast	Rain	Night	Snow	Sun	Dusk	Overcast	Rain	Night	Snow	Sun	Dusk	Overcast	Rain	Night	Snow
	Mode ↓																		
Sun	RGB	—	52.0	94.4	92.5	27.1	81.7	—	49.3	95.1	90.9	21.4	82.2	—	45.0	95.8	93.7	22.1	84.2
	Gray	—	56.7	95.1	93.5	49.6	84.6	—	55.5	95.4	92.7	48.8	84.5	—	57.7	96.0	93.6	55.4	85.1
Dusk	RGB	48.1	—	48.9	45.0	21.4	51.2	47.6	—	46.6	44.6	17.6	50.1	41.1	—	37.5	39.1	13.2	44.9
	Gray	52.3	—	52.1	48.6	39.0	55.7	52.6	—	52.7	48.3	38.0	53.9	50.8	—	52.0	48.3	38.6	54.4
Overcast	RGB	95.2	53.8	—	92.2	29.5	84.1	94.7	50.4	—	91.0	25.6	84.4	95.2	47.6	—	93.4	25.1	86.2
	Gray	94.5	58.5	—	93.8	56.3	87.8	95.2	58.2	—	93.4	54.0	87.8	95.8	59.1	—	94.3	58.8	87.7
Rain	RGB	88.3	46.7	89.6	—	22.9	73.8	87.5	44.8	90.0	—	22.1	73.7	90.6	43.2	91.2	—	18.8	76.3
	Gray	92.7	49.6	92.6	—	46.0	79.3	93.0	49.9	92.5	—	44.9	80.2	93.1	50.6	93.6	—	48.2	81.2
Night	RGB	35.0	31.5	35.3	29.7	—	27.8	30.6	31.0	32.7	31.9	—	28.0	34.0	27.5	34.0	28.8	—	28.1
	Gray	57.6	47.6	61.7	52.3	—	52.7	55.8	46.5	59.8	52.2	—	48.3	57.8	45.7	60.5	54.7	—	53.6
Snow	RGB	84.1	60.3	88.2	79.3	26.3	—	83.5	56.7	87.2	78.2	24.0	—	87.6	55.5	90.7	82.0	21.4	—
	Gray	85.8	61.9	89.8	83.4	45.2	—	87.5	62.1	89.8	82.5	45.8	—	87.7	64.8	91.0	84.7	53.6	—
Avg. ΔR@1 (RGB-Gray)		-9.3						-10.3						-12.5					

TABLE XIII
RECALL@1 ACROSS DATASETS WITH MIXVPR TRAINED & EVALUATED ON THE SAME MODALITY, WITHOUT PRETRAINING.

Model	Mode	Pitts250k (Test)	SPED	GLDv2	Tokyo247	Avg.ΔR@1 (RGB-Gray)
MixVPR (ResNet18)	RGB	91.5	72.7	40.2	62.2	0.2
	Gray	91.4	78.3	39.2	56.8	
MixVPR (ResNet34)	RGB	90.8	72.0	39.5	56.2	0.4
	Gray	89.9	76.8	37.8	52.4	
MixVPR (ResNet50)	RGB	90.3	66.9	41.3	54.6	-1.4
	Gray	90.8	73.1	40.0	54.6	

der challenging VPR conditions. Notably, MixVPR-ResNet18 fine-tuned on grayscale sometimes outperforms its ResNet50 RGB counterpart, demonstrating that the robustness gains from grayscale can compensate for a shallower model. Pitts250k and Tokyo24/7 show little sensitivity to VPR input modality, likely reflecting their focus on viewpoint variation over appearance shift, where color remains more consistent. In contrast, SPED consistently benefits from grayscale VPR, while GLDv2 consistently favors RGB, again highlighting that chromatic utility is dependent on the stability and prevalence of color cues in the environment. Generally, from Fig. 3, we see that RGB training offers no significant overall advantage over grayscale across MixVPR configurations.

3) Gray-Pretrained MixVPR. With a grayscale-pretrained backbone, grayscale VPR fine-tuning consistently outperforms its RGB counterpart across all datasets and backbone sizes

(Tables VIII to X), with the most pronounced gains on appearance-challenging conditions such as Nordland winter and Oxford RobotCar night. As in setup 2, we see that grayscale VPR with ResNet18 can outperform RGB VPR with ResNet50. From Fig. 3, fully grayscale-trained MixVPR performs competitively and can outperform both off-the-shelf and fully RGB-trained variants across benchmarks. However, with GLDv2, RGB-pretraining maintains a marginal advantage of up to 2%, consistent with its stable landmark-oriented color cues. These results demonstrate that the advantage of color is context-dependent, but limited, making fully grayscale-trained models a compelling and robust alternative for VPR.

4) MixVPR - No Pretraining As expected, removing ImageNet pretraining reduces performance across all cases (see Fig. 3), emphasizing the value of low-level features learned through foundation model pretraining. Nevertheless, from Tables XI to XIII, grayscale VPR-only training often outperforms its RGB counterpart, particularly on appearance-challenging datasets, averaging up to 6.3% R@1 gain on Nordland and 12.5% on Oxford RobotCar. This suggests that GSV-Cities alone, despite its scale, does not provide sufficient color invariance for robust generalization under the severe appearance shifts present in VPR benchmarks. By removing color, the model is encouraged to prioritize luminance-based structure during training, which remain more

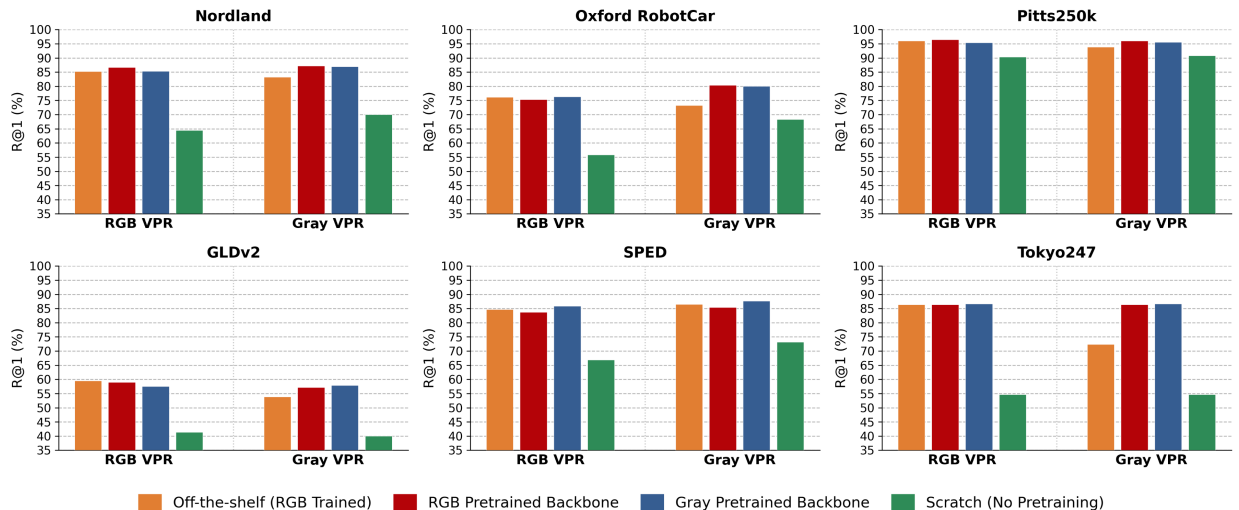


Fig. 3. Recall@1 on MixVPR (ResNet50) across the four setups from Fig. 2. Nordland and Oxford RobotCar results are averaged across season and condition pairs respectively. RGB/Gray VPR denote the training and evaluation modality, except setup 1 where off-the-shelf models are evaluated per modality only.

stable across appearance conditions. Following the previous setups, performance on Pitts250k remains largely unaffected by input modality, while SPED, GLDv2 and Tokyo24/7 show more variable responses, reflecting greater sensitivity to input modality without the stability provided from pretraining, and a trade-off between structural cues and consistent chromatic features present within the data.

V. DISCUSSION

Structure is sufficient for global VPR. Across evaluations, grayscale models match or outperform their RGB counterparts, with even fully RGB-trained ViT models differing minimally under color removal, reinforcing that luminance-based structure is the driving factor in global place recognition.

Color volatility can mislead models. Color is inherently unstable under appearance shifts, and RGB training can encourage misleading correlations between chromatic cues and places (models without as-extensive pretraining, such as MixVPR, become over-reliant on color features), underperforming their more robust grayscale versions under extreme conditions. Stronger pretraining like in BoQ stabilizes performance across both modes, with grayscale remaining competitive throughout.

Color is context-dependent. Color benefit, generally within 1-4% R@1, is observed in landmark-focused data where color cues are consistent and prevalent with fewer appearance changes. Nevertheless, structure remains the dominant factor of robust performance.

Computational Implications. Color imagery incurs three times the storage and data movement cost of grayscale. This is increasingly relevant as recent VPR methods rely on large-scale training. Datasets such as GSV-Cities (~23GB), MSLS (196GB cache requirement for NetVLAD representations [29]) and SF-XL (~1TB) highlight the overhead that increases when color invariance is incomplete and augmentation or dataset ensembling is required.

During training, GPU memory is dominated by activations and gradients. Large models such as MegaLoc (228M parameters) report 60GB VRAM usage, requiring batch processing

with continuous host-to-device transfer. Such operations make data loading a known bottleneck. While forward and backward pass costs are largely unaffected by channel reduction, single-channel data reduces storage and transfer volume. Across multiple MixVPR training runs, we measured a consistent 29% reduction in peak RAM utilization across all ResNet backbone sizes and $\sim 1.5\times$ lower CPU utilization, reflecting reduced loader overhead from decoding, decompressing and transferring batches, and leaving headroom for larger batch sizes or concurrent processes.

Grayscale is also particularly well-suited to TinyML and resource-constrained deployment [30], where micro-controllers operate under 256KB-1MB SRAM budgets. Reducing input tensor size lowers buffering and data movement costs, consistent with benchmarks such as Visual Wake Words and FashionMNIST which use low-resolution or single-channel inputs. Our results show that smaller grayscale-trained backbones can match or outperform larger RGB variants, enabling a practical model-size trade-off. Grayscale further aligns with low-bit embedded sensor modalities common in robotics, such as monochrome, thermal, depth and event cameras, with monochrome cameras additionally avoiding demosaicing overhead and offering improved light sensitivity under low-light conditions that challenge VPR systems.

VI. CONCLUSION

We investigate the role of color in VPR across training regimes and model architectures. RGB imagery offers limited advantage over grayscale under current SotA conventions, with structure and texture forming the foundation of global VPR performance. Grayscale can even outperform RGB under severe appearance shifts where color is volatile and invariance insufficiently learned. Where persistent chromatic cues exist, RGB may provide support, which is more relevant for landmark-focused retrieval. For deployment, grayscale reduces storage and transfer overhead, improving training efficiency and suiting resource-constrained platforms, making it a practical and compelling default modality for VPR.

Limitations and Future Work. Extending this analysis to transformer-based training remains important, though models such as BoQ already show near-identical RGB and grayscale performance off-the-shelf, suggesting a grayscale-trained variant could likely match or surpass RGB under challenging conditions. Future work includes real-world deployment evaluations across hardware settings and further investigation into model and training design under grayscale input.

REFERENCES

- [1] G. Berton, G. Trivigno, B. Caputo, and C. Masone, "Eigenplaces: Training viewpoint robust models for visual place recognition," in *2023 IEEE/CVF International Conference on Computer Vision (ICCV)*, 2023, pp. 11 046–11 056.
- [2] G. Berton, C. Masone, and B. Caputo, "Rethinking visual geolocalization for large-scale applications," in *2022 IEEE/CVF Conference on Computer Vision and Pattern Recognition (CVPR)*, 2022, pp. 4868–4878.
- [3] R. Arandjelovic, P. Gronat, A. Torii, T. Pajdla, and J. Sivic, "Netvlad: Cnn architecture for weakly supervised place recognition," in *2016 IEEE Conference on Computer Vision and Pattern Recognition (CVPR)*, 2016, pp. 5297–5307.
- [4] A. Ali-Bey, B. Chaib-Draa, and P. Giguère, "Mixvpr: Feature mixing for visual place recognition," in *2023 IEEE/CVF Winter Conference on Applications of Computer Vision (WACV)*, 2023, pp. 2997–3006.
- [5] F. Lu, X. Lan, L. Zhang, D. Jiang, Y. Wang, and C. Yuan, "Cricavpr: Cross-image correlation-aware representation learning for visual place recognition," in *2024 IEEE/CVF Conference on Computer Vision and Pattern Recognition (CVPR)*, 2024, pp. 16 772–16 782.
- [6] G. Berton and C. Masone, "Megaloc: One retrieval to place them all," in *2025 IEEE/CVF Conference on Computer Vision and Pattern Recognition Workshops (CVPRW)*, 2025, pp. 2852–2858.
- [7] A. Ali-bey, B. Chaib-draa, and P. Giguère, "Gsv-cities: Toward appropriate supervised visual place recognition," *Neurocomput.*, vol. 513, no. C, p. 194–203, Nov. 2022.
- [8] A. Torii, J. Sivic, T. Pajdla, and M. Okutomi, "Visual place recognition with repetitive structures," in *2013 IEEE Conference on Computer Vision and Pattern Recognition*, 2013, pp. 883–890.
- [9] D. M. Chen, G. Baatz, K. Köser, S. S. Tsai, R. Vedantham, T. Pylvänäinen, K. Roimela, X. Chen, J. Bach, M. Pollefeys, B. Girod, and R. Grzeszczuk, "City-scale landmark identification on mobile devices," in *CVPR 2011*, 2011, pp. 737–744.
- [10] A. Singh, A. Bay, and A. Mirabile, "Assessing the importance of colours for cnns in object recognition," in *NeurIPS 2020 Workshop on Shared Visual Representations in Human and Machine Intelligence (SVRHM)*, 2020.
- [11] M. Vogelsang, L. Vogelsang, P. Gupta, T. K. Gandhi, P. Shah, P. Swami, S. Gilad-Gutnick, S. Ben-Ami, S. Diamond, S. Ganesh, and P. Sinha, "Impact of early visual experience on later usage of color cues," *Science*, vol. 384, no. 6698, pp. 907–912, 2024.
- [12] I. Bramão, A. Reis, K. M. Petersson, and L. Fafsa, "The role of color information on object recognition: A review and meta-analysis," *Acta Psychologica*, vol. 138, no. 1, pp. 244–253, 2011.
- [13] P. Brosseau, A. Nestor, and M. Behrmann, "Colour blindness adversely impacts face recognition," *Visual Cognition*, vol. 28, no. 4, pp. 279–284, 2020.
- [14] C. Breuil, B. J. Jennings, S. Barthelmé, N. Guyader, and F. A. A. Kingdom, "Color improves edge classification in human vision," *PLOS Computational Biology*, vol. 15, no. 10, pp. 1–15, 10 2019.
- [15] A. Bhatta, D. Mery, H. Wu, J. Annan, M. C. King, and K. W. Bowyer, "What's color got to do with it? face recognition in grayscale," *IEEE Transactions on Biometrics, Behavior, and Identity Science*, vol. 7, no. 3, pp. 484–497, 2025.
- [16] V. Buhrmester, D. Münch, D. Bulatov, and M. Arens, "Evaluating the impact of color information in deep neural networks," in *Pattern Recognition and Image Analysis*, A. Morales, J. Fierrez, J. S. Sánchez, and B. Ribeiro, Eds. Cham: Springer International Publishing, 2019, pp. 302–316.
- [17] A. Y. J. Yao and W. Einhäuser, "Color aids late but not early stages of rapid natural scene recognition," *Journal of Vision*, vol. 8, no. 16, pp. 12–12, 12 2008.
- [18] A. Delorme, G. Richard, and M. Fabre-Thorpe, "Ultra-rapid categorisation of natural scenes does not rely on colour cues: a study in monkeys and humans," *Vision Research*, vol. 40, no. 16, pp. 2187–2200, 2000.
- [19] A. W. Yip and P. Sinha, "Contribution of color to face recognition," *Perception*, vol. 31, no. 8, pp. 995–1003, 2002, PMID: 12269592.
- [20] K. A. Ehinger and J. R. Brockmole, "The role of color in visual search in real-world scenes: Evidence from contextual cuing," *Perception & Psychophysics*, vol. 70, no. 7, pp. 1366–1378, Oct 2008.
- [21] S. Izquierdo and J. Civera, "Optimal transport aggregation for visual place recognition," in *Proceedings of the IEEE/CVF Conference on Computer Vision and Pattern Recognition (CVPR)*, June 2024.
- [22] A. Ali-bey, B. Chaib-draa, and P. Giguère, "BoQ: A place is worth a bag of learnable queries," in *Proceedings of the IEEE/CVF Conference on Computer Vision and Pattern Recognition (CVPR)*, June 2024, pp. 17 794–17 803.
- [23] D. G. Lowe, "Distinctive image features from scale-invariant keypoints," *Int. J. Comput. Vision*, vol. 60, no. 2, p. 91–110, Nov. 2004.
- [24] E. Rublee, V. Rabaud, K. Konolige, and G. Bradski, "Orb: An efficient alternative to sift or surf," in *2011 International Conference on Computer Vision*, 2011, pp. 2564–2571.
- [25] H. Jégou, M. Douze, C. Schmid, and P. Pérez, "Aggregating local descriptors into a compact image representation," in *2010 IEEE Computer Society Conference on Computer Vision and Pattern Recognition*, 2010, pp. 3304–3311.
- [26] J. Sivic and A. Zisserman, "Efficient visual search of videos cast as text retrieval," *IEEE Transactions on Pattern Analysis and Machine Intelligence*, vol. 31, no. 4, pp. 591–606, 2009.
- [27] F. Radenović, G. Toliás, and O. Chum, "Fine-tuning cnn image retrieval with no human annotation," *IEEE transactions on pattern analysis and machine intelligence*, vol. 41, no. 7, pp. 1655–1668, 2018.
- [28] S. Izquierdo and J. Civera, "Close, but not there: Boosting geographic distance sensitivity in visual place recognition," in *Computer Vision – ECCV 2024: 18th European Conference, Milan, Italy, September 29–October 4, 2024, Proceedings, Part LXXIII*. Berlin, Heidelberg: Springer-Verlag, 2024, p. 240–257.
- [29] A. Ali-Bey, B. Chaib-draa, and P. Giguère, "Global proxy-based hard mining for visual place recognition," in *33rd British Machine Vision Conference 2022, BMVC 2022, London, UK, November 21-24, 2022*. BMVA Press, 2022.
- [30] J. Lin, L. Zhu, W.-M. Chen, W.-C. Wang, and S. Han, "Tiny machine learning: Progress and futures [feature]," *IEEE Circuits and Systems Magazine*, vol. 23, no. 3, pp. 8–34, 2023.
- [31] B. Şimşek and H. Ş. Bilge, "A novel motion blur resistant vSLAM framework for Micro/Nano-UAVs," *Drones*, vol. 5, no. 4, 2021.
- [32] J. Kim, Y. Cho, and S. Yoon, "Towards test-time efficient visual place recognition via asymmetric query processing," *Proceedings of the AAAI Conference on Artificial Intelligence*, vol. 40, no. 7, pp. 5673–5681, 2026, publisher Copyright: © 2026, Association for the Advancement of Artificial Intelligence (www.aaai.org). All rights reserved.; 40th AAAI Conference on Artificial Intelligence, AAAI 2026 ; Conference date: 20-01-2026 Through 27-01-2026.
- [33] T. C. Nijboer, R. Kanai, E. H. de Haan, and M. J. van der Smagt, "Recognising the forest, but not the trees: An effect of colour on scene perception and recognition," *Consciousness and Cognition*, vol. 17, no. 3, pp. 741–752, 2008.
- [34] M. Engilberge, E. Collins, and S. Süsstrunk, "Color representation in deep neural networks," in *2017 IEEE International Conference on Image Processing (ICIP)*, 2017, pp. 2786–2790.
- [35] M.-C. Chiu, Y. Wang, D. E. G. Kim, P.-Y. Chen, and X. Ma, "Colorsense: A study on color vision in machine visual recognition," in *2025 IEEE Conference on Secure and Trustworthy Machine Learning (SaTML)*, 2025, pp. 681–697.
- [36] K. De and M. Pedersen, "Impact of colour on robustness of deep neural networks," in *2021 IEEE/CVF International Conference on Computer Vision Workshops (ICCVW)*, 2021, pp. 21–30.
- [37] T. Ismagilov, B. Ferrarini, M. Milford, N. Tan Viet Tuyen, S. D. Ramchurn, and S. Ehsan, "On motion blur and deblurring in visual place recognition," *IEEE Robotics and Automation Letters*, vol. 10, no. 5, pp. 4746–4753, 2025.
- [38] S. Garg, N. Suenderhauf, and M. Milford, "Don't look back: Robustifying place categorization for viewpoint- and condition-invariant place recognition," in *2018 IEEE International Conference on Robotics and Automation (ICRA)*, 2018, pp. 3645–3652.
- [39] M. Zaffar, S. Garg, M. Milford, J. Kooij, D. Flynn, K. McDonald-Maier, and S. Ehsan, "Vpr-bench: An open-source visual place recognition evaluation framework with quantifiable viewpoint and appearance change," *International Journal of Computer Vision*, pp. 1–39, 2021.
- [40] C. Masone and B. Caputo, "A survey on deep visual place recognition," *IEEE Access*, vol. 9, pp. 19 516–19 547, 2021.